

X-ray investigation of the smectic *A* reentrant nematic transition under pressure (CBOOA)

D. Guillon\* and P. E. Cladis  
Bell Laboratories, Murray Hill, New Jersey 07974

D. Aadsen and W. B. Daniels  
Department of Physics, University of Delaware, Newark, Delaware 19711  
(Received 11 July 1979)

The authors present the first x-ray measurement of the liquid crystal smectic *A* phase layer spacing at high pressure. It is found that at relatively high temperatures, when the smectic *A* phase is compressed toward the reentrant nematic phase, there is no change in the layer spacing. On the other hand, at lower temperatures, where the smectic *A* phase is being compressed toward the stable solid phase, the layer spacing decreases. A systematic increase in the layer spacing as a function of time is also noted.

## I. INTRODUCTION

A few years ago, Cladis<sup>1</sup> observed a "reentrant" nematic phase for a mixture of two liquid crystals. That is, by decreasing the temperature from the nematic phase, she identified (using the light microscope) the following sequence of phases: nematic, smectic, nematic. More recently Cladis *et al.*<sup>2</sup> have demonstrated the existence of the same reentrant nematic-phase property for pure compounds under pressure. In this case (as may be seen by reference to Fig. 1), starting from the nematic phase at one atmosphere, one observes with increasing pressure the same sequence of phases as reported above. Fig. 1 shows the schematic diagrams (*T*, conc.), (*P*, *T*) for a mixture and for a pure compound, in which this reentrant nematic phase occurs.

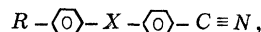
Although counterintuitive, the reentrant nematic phase does not violate any laws of thermodynamics<sup>3</sup> and can apparently be described within the framework of a Landau theory.<sup>4</sup>

The study of liquid crystals under pressure has developed considerably in the past few years. Several techniques have been used, such as nuclear magnetic resonance,<sup>5</sup> microscopy<sup>2,6,7</sup> and differential thermal analysis.<sup>8</sup> The identification of the different mesomorphic phases which can be observed as a function of pressure has been made, either by observation of textures in the case of microscopy, or deduced by continuity of the lines of transition in the phase diagram to low pressures for the case of the differential thermal analysis.<sup>8</sup> This paper reports a study of liquid crystals under pressure using x-ray diffraction. The x-ray technique permits a clear identification of the phases, for it gives directly the relevant structural parameters, which are well specified for each mesomorphic phase. Moreover, it gives information on the evolution of the structural

parameters as functions of pressure and temperature.

We will present in this paper the x-ray investigation of the reentrant phenomenon. Initial x-ray studies have been made on mixtures of liquid crystals at one atmosphere and have been described elsewhere.<sup>7</sup> The present results were obtained by compression of a pure compound.

The reentrant phenomenon has only been observed with cyanocompounds, the chemical constitution of which can be schematically represented as follows:



where *X* is N=CH or CH=N and *R* is C<sub>*n*</sub>H<sub>2*n*+1</sub> or O-C<sub>*n*</sub>H<sub>2*n*+1</sub>.

These compounds have a very strong dipole (4.5 d) at one end of their polar part.<sup>9</sup> A model, has been proposed for the organization of this type of molecule in the smectic *A* phase and in the reentrant nematic phase.<sup>10</sup> In this model, which is represented in Fig. 2, the molecules are assumed to be associated in antiparallel pairs. This model leads to weak forces between the dif-

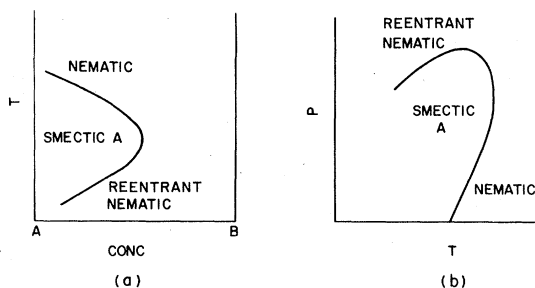


FIG. 1. Schematic drawings of the reentrant nematic phase: (a) with a mixture of two-liquid crystal compounds *A* and *B* as a function of concentration at one atmosphere; (b) with a pure compound as a function of pressure and temperature.

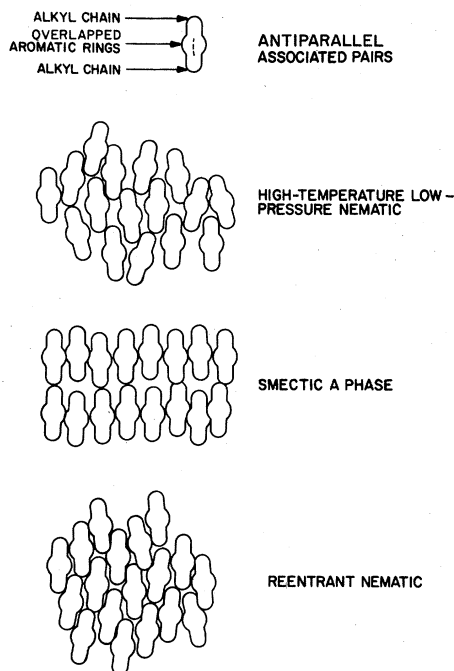


FIG. 2. Schematic arrangement of antiparallel associated pairs in the nematic, smectic *A*, and reentrant nematic phase.

ferent polar parts of the pairs because of the neutralization of the large cyano dipole. Thus the *pair* is not so strongly differentiated into polar and nonpolar segments as the single molecule. In this case, applying pressure can deform and compress the molten aliphatic chains, and when the interaromatic spacing in a direction parallel to the plane of the layers becomes small enough, so that the interaromatic forces are strongly repulsive, a buckling destabilization of the layers can occur as the pairs seek to fill up empty spaces of the structure in a more efficient packing. In this paper we will report the results we have obtained in the smectic *A* phase and in the reentrant nematic phase of a pure cyanocompound as functions of pressure and temperature using x-ray diffraction techniques.

We have found that the high-pressure reentrant nematic phase induced in pure *N-p*-cyanobenzylidene-*p*-octyloxyaniline (CBOOA) appears microscopically identical to the classical low-pressure nematic. We have also found that the change in the layer spacing in the smectic *A* phase is very small as the compound is compressed toward the reentrant nematic phase. Finally, we have found that the reentrant nematic phase crystallizes to a spacing of 19–20 Å rather than the usual 26 Å of the stable solid phase at 1 atmosphere.

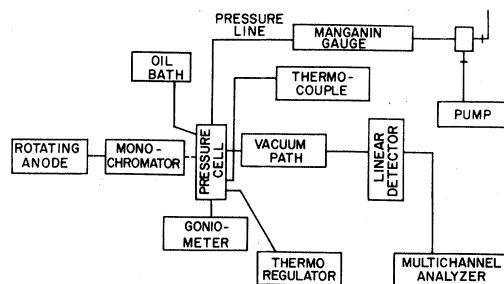


FIG. 3. Experimental setup (see text).

## II. APPARATUS AND TECHNIQUE

### A. Apparatus and sample

Our experimental setup is schematically represented in Fig. 3. We have used an x-ray-diffraction system equipped with a rotating anode and a bent quartz crystal. The patterns are registered with a stable position-sensitive x-ray detector. This apparatus has been described in more detail previously.<sup>11</sup>

A schematic drawing of the cell is presented in Fig. 4. The pressure cell consists of two connected parts. The first part, a, contains the pressurizing fluid; the second part, b, is machined from type 7075-T6 aircraft aluminum alloy into which a  $\frac{1}{4}$ -in. o.d.,  $\frac{1}{16}$ -in. i.d. beryllium cylinder represents the critical component of the pressure cell and contains the sample which is seen by the x-ray beam. In the sample space of the beryllium cylinder is a quartz capillary (10- $\mu$  thick) which has been previously treated

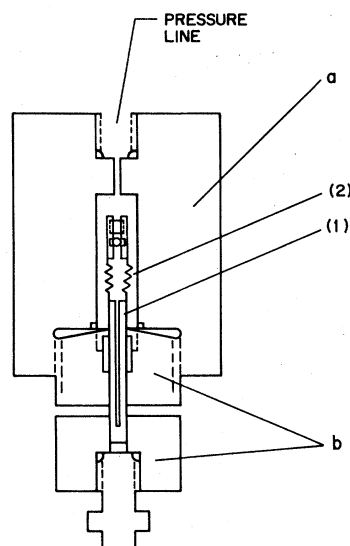


FIG. 4. Pressure cell. See text for details of the different parts.

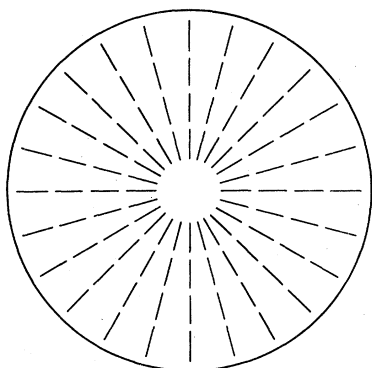


FIG. 5. Arrangement of the molecules in the capillary inside the beryllium cylinder. The long-range orientational order is radial at the walls of the capillary.

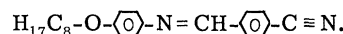
with a surfactant.<sup>12</sup> Thus the part of the sample which is irradiated by the x-ray beam is oriented, and the long-range orientational order is radial at the walls, as shown in Fig. 5. A flexible Teflon bellows ([2] in Fig. 4) also filled with the sample is attached to the upper part of the beryllium cylinder to separate the liquid-crystal sample from the pressurizing fluid.

The orientation of the sample is highly advantageous, for it allows us to have a very well-defined diffracted x-ray beam. Even though the beryllium part absorbs 80% of the x-ray beam, we have been able to obtain well-defined patterns in a few minutes. Typically, all our experimental data have been collected with patterns using exposure times of about 20 min. The success of the method is largely due to the high flux and the multichannel detection of the linear position-sensitive detector. In this case, the number of counts was sufficient to draw quantitative conclusions. The precision on the spacings we have determined is of the order of 0.1 Å, as indicated by the reproducibility of the measurements which will be represented later.

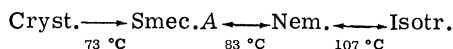
The pressurizing fluid is octoil S. [Octoil S ≡ "Plexol 201" from Rohm and Haas Co. (Philadelphia).] High pressures have been generated by means of a hand pump and measured with a Manganin gauge. The reading of the pressure is better than 0.5 bar. The stability of the pressure inside the cell depends on the temperature stability. The latter was sufficient to ensure a pressure which did not vary by more than 0.5 bar during the exposure time of one pattern.

Part a of the cell was heated with a surrounding coil in which oil circulates. Part b was heated by an electric wire wrapped around its exterior. The temperature was measured by a thermocouple glued onto the outside of the beryllium core as near as possible to the sample.

We have used two samples of the same cyano-compound *N-p*-benzylidene-*p*-octyloxyaniline:



This liquid crystal is known to have the following sequence of phases on increasing temperature at one atmosphere:



The two samples were purchased from Eastman Kodak Company. The first was used without further purification. The second one was recrystallized three times before filling the cell.

### B. Typical patterns

Figure 6 shows two patterns obtained with CBOOA as a function of pressure. At 1 atm in the nematic phase we observe a diffuse peak which is characteristic of the smectic fluctuations in the nematic phase. This nematic peak corresponds to a density wave spacing which is of the order of magnitude of the layer spacing in the smectic A

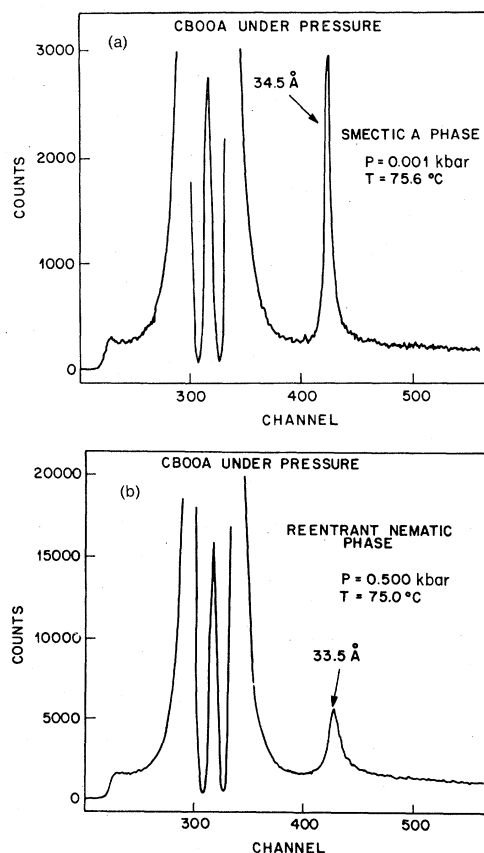


FIG. 6. (a) Example of a typical smectic A pattern obtained with the pressure cell. (b) Example of a typical reentrant nematic phase obtained with the same cell.

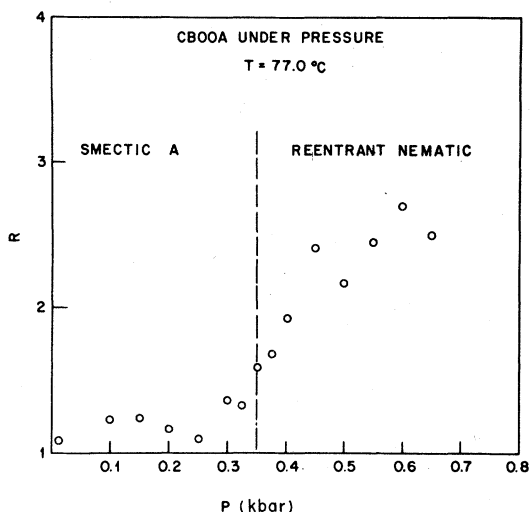


FIG. 7.  $R$  as a function of pressure.  $R = [\text{width at half maximum of smectic (nematic) peak}] / [\text{width at half maximum of central beam}]$ . In the smectic  $A$  phase  $R$  is very close to 1, since the width of the smectic peak is very close to the experimental resolution. In the reentrant nematic phase  $R$  is much larger, since the reentrant nematic peak is diffuse as is the classical nematic peak.

phase. The smectic  $A$  phase 6(a) is characterized by a sharp peak. In the reentrant nematic phase 6(b) a diffuse peak is observed at the same position. The remainder of the pattern is due to the central beam together with the diffracted beams from the beam stop and the beryllium. As can be seen from this figure, one can easily fix the transition points between smectic and nematic phases by observation of the width of the peak at the half maximum. In the nematic phase, the width is larger than the central beam, while in the smectic phase it is essentially as narrow as the central beam (resolution limited).

Figure 7 shows the variation of the width of the smectic and nematic peaks (normalized to the width of the central beam) as a function of pressure. The transition pressure at this temperature is marked by the vertical dashed line.

### III. EXPERIMENTAL RESULTS

#### A. First sample

Figure 8 shows the variation of the space as a function of pressure observed in the smectic  $A$  phase and in the reentrant nematic phase. We have plotted three consecutive runs: increasing, then decreasing, and again increasing pressure. The reproducibility of the phenomenon is very good, and apparently, there is no hysteresis in the variation of the spacing.

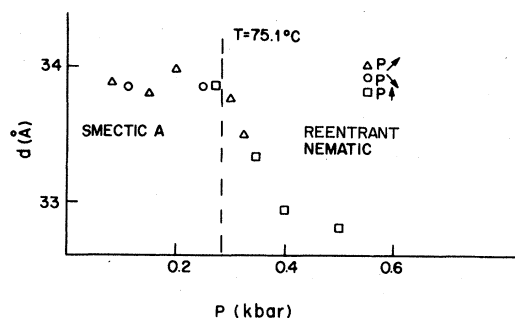


FIG. 8. Change in the layer spacing as a function of pressure. We show three consecutive runs:  $\Delta \equiv$  increasing pressure;  $\circ \equiv$  decreasing pressure, and  $\square \equiv$  increasing again pressure. The smectic  $A$  layer spacing is constant.

The variation of the spacing from one other run at different temperatures is shown in Fig. 9. From this figure, we can see that the layer spacing is nearly constant within the smectic  $A$  phase with increasing pressure. This is a remarkable and interesting feature. We will discuss it later. In the nematic phase, the spacing decreases slowly with increasing pressure.

Finally, in Fig. 10, we have represented all the runs we have collected as a function of pressure for this sample. First, we can note that as the sample ages (on a time scale of days), the pressure of the transition between the smectic phase and the reentrant nematic increases slowly with the pressure. The second important feature is the increase of the layer spacing in the smectic  $A$  phase as a function of time. A third feature is that the layer spacing in the smectic  $A$  phase is stable each time we obtain the reentrant nematic phase at high pressure. The first and the second features can be explained by a shift of the boundary line between the smectic phase and the nematic one in the  $(P, T)$  plane. This shift would be caused by the presence of impurity, or by the

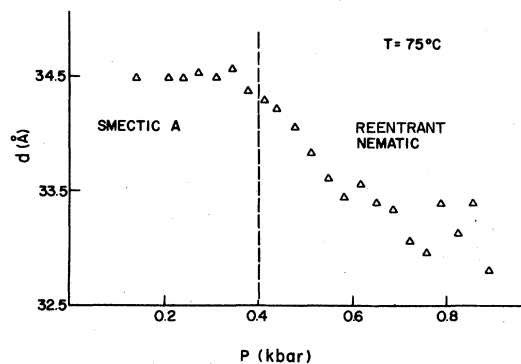


FIG. 9. The layer spacing as a function of pressure for sample  $A$ .

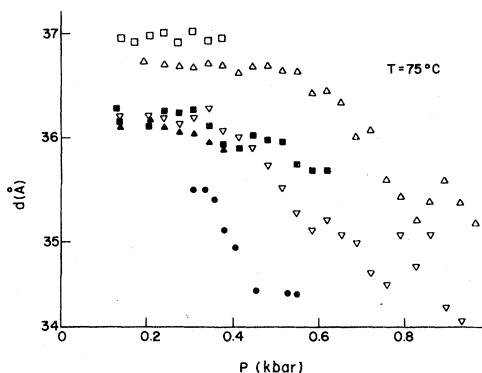


FIG. 10. All the layer spacing data collected for sample A as a function of pressure. The chronological order of the different runs is the following: ● = Run 1; ▲ = Run 2; ▽ = Run 3; ■ = Run 4; △ = Run 5; and □ = Run 6.

degradation of the sample with the time. It is well known that the Schiff's bases in general are very difficult to keep in a high degree of purity, when they are heated in the nematic phase. On the other hand, it has been demonstrated<sup>10</sup> that the shape of the  $(P, T)$  diagram is very sensitive to the purity of the sample.

Once the reentrant nematic phase is obtained by applying a higher pressure, we reach a value of the pressure for which the sample crystallizes. In the case of this sample this was at about 1 kbar. Occurrence of crystallization is easily observed by the accompanying pressure drop due to the change in the sample volume. The crystal patterns we observe have the following spacings: 20.1 and 18.6 Å. It is worth comparing these spacings with those obtained in the case of the reentrant nematic phase with mixtures.<sup>7</sup> In this case for example, for a mixture of *p*-hexyloxybenzylidene-*p*-aminobenzonitrile (HBAB) in CBOOA, it has been shown that we can stabilize the sample in a state where the reentrant nematic phase coexists a very long time with a crystalline phase which has a characteristic spacing of about 19 Å. This corresponds to the distance between two antiparallel pairs as proposed in the model of organization of the cyano compounds in Fig. 2.<sup>10</sup> This crystalline form (crystal B) is not the stable one (crystal A) usually observed for CBOOA; at room temperature this sample has a crystalline packing with a layer of 25 Å (crystal A).

If we continue to apply pressure up to 3 kbar, the crystalline pattern stays the same, and there is no noticeable change in the observed spacings. But by decreasing the temperature at constant pressure (2 kbar), there is a transition to the stable crystal A with the 25-Å spacing.

We have represented in Fig. 11 the variation of

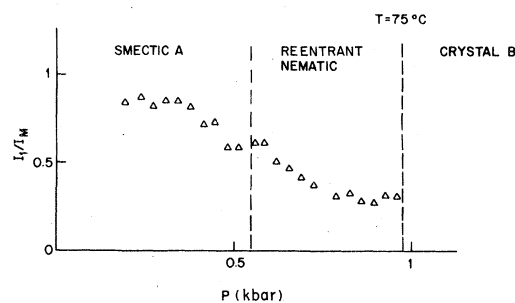


FIG. 11.  $I_1/I_m$  = (intensity of Bragg peak)/(intensity of central beam). This is shown for sample A as a function of pressure. The intensities have been obtained by integrating over a fixed number of channels for  $I_1$  and  $I_m$ .

the scattered intensity as a function of the pressure in the smectic A phase and in the reentrant nematic one. From this figure we see a decrease of scattered intensity in the smectic A phase upon approaching the transition to the reentrant nematic phase. This behavior is similar to that observed by McMillan in reporting<sup>13</sup> his experiments on the smectic A phase of cholesteryl nonanoate. In the reentrant nematic phase, the scattered intensity continues to decrease as a function of pressure down to a certain level, where it seems to stabilize.

If we look now at Fig. 12, we see that the inverse of the width at the half maximum of the peak in the reentrant nematic phase decreases linearly with increasing pressure down to a level where it stabilizes. Assuming a Gaussian approximation for the peak in the nematic, we can calculate the number of molecules which are correlated. That number is represented in Fig. 13 as a function of pressure.

Apparently, there are two regions in the be-

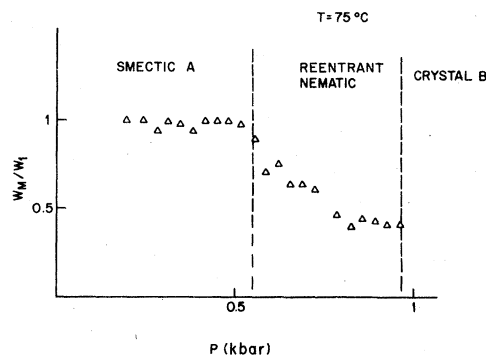


FIG. 12. The inverse of the width of the low-angle Bragg peak at the half maximum as a function of pressure for sample A.  $W_m$  = width of central beam.  $W_1$  = width of Bragg peak. We have used the same number of channels as in Fig. 11.

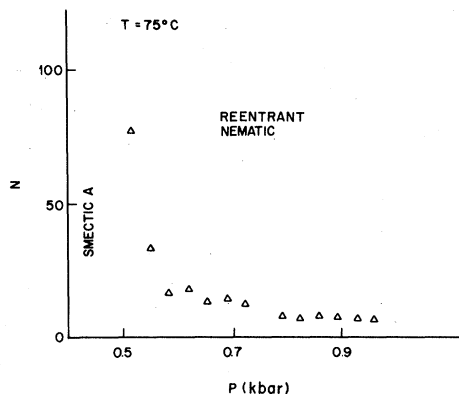


FIG. 13. Number of molecules correlated in the direction normal to the layers (calculated from a Gaussian approximation) as a function of pressure. This number reflects the number of "layers" in the cybotactic cluster.

havior of the reentrant nematic phase; the first, which is the closest to the transition to the smectic A phase, is very similar in behavior to a classical nematic as a function of temperature in the vicinity of a smectic A phase. The second occurs at high pressure, where the organization of the molecules seems blocked (the intensity and the width of the peak stay the same above 0.8 kbar).

#### B. Second sample

We have represented in Fig. 14 the variation of the spacing for this sample. The temperature in this case is 77 °C. We observe the same behavior as for the previous sample. The transition between the smectic A phase and the reentrant nematic occurs around 400 bar, although this sample apparently is purer than the first one.

Figures 15 and 16, which represent respectively the variation of the scattered intensity as a function of pressure, and the evolution of the inverse of the width of the peak as a function of

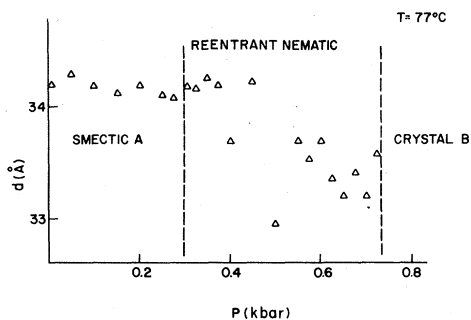


FIG. 14. Change in the layer spacing (corresponding to the low-angle Bragg peak) as a function of pressure for sample B.

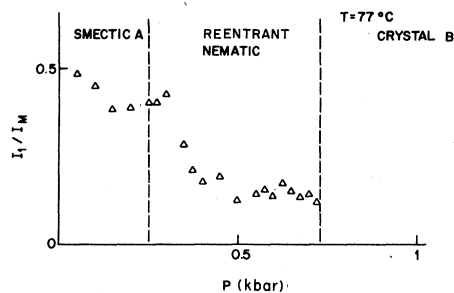


FIG. 15. The scattered intensity of the low-angle Bragg peak as a function of pressure for sample B. The experimental determination is the same as indicated in Fig. 11.

pressure, are very similar to the figures for sample A. In the reentrant nematic we note also a decrease in the scattered intensity down to a certain level where it seems to stabilize. For the inverse of the width, we see also the same kind of behavior. Thus for temperatures above 72 °C, this sample behaves like the first one. For temperatures below 72 °C, where we are now compressing the smectic A toward a solid phase rather than a reentrant nematic phase, we observe a spacing which decreases with increasing pressure as shown in Fig. 17 for  $T = 69$  °C and 65.8 °C. This behavior is perfectly reversible. For example, at 69 °C, by taking data again after increasing the pressure, we find the same value of the layer spacing as at the beginning of the run. That means that the decrease in the layer spacing is quite real. We have reported in the figure the slopes of the regression lines which have been calculated by a least-squares fit of the experimental data. Another important feature is that at these temperatures, it was impossible to obtain the reentrant nematic phase; the sample crystallizes in the stable form with a layer spacing of about 25 Å.

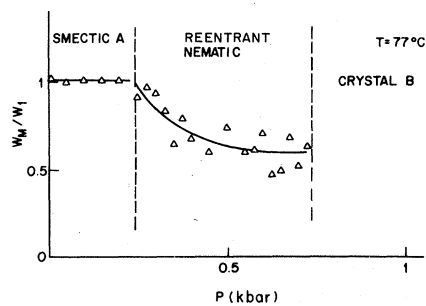


FIG. 16. The inverse of the width of the low-angle Bragg peak at the half maximum as a function of pressure for sample B. The experimental determination is the same as indicated in Fig. 12. The line is a guide for the eye.

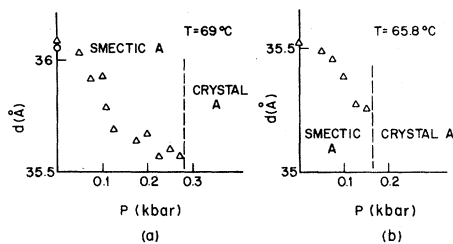


FIG. 17. Evolution of the layer spacing in the smectic A phase for two temperatures. (a) the point (O) has been taken after the run of increasing pressure and coming back to one atmosphere. The decrease of the layer spacing can be expressed as  $d (\text{Å}) = 36.06 (\text{Å}) - 2.067 P (\text{kbar})$ . (b) The decrease of the layer spacing can be expressed as  $d (\text{Å}) = 35.62 (\text{Å}) - 2.262 P (\text{kbar})$ .

#### IV. SUMMARY AND COMMENTS

##### A. Changes in the smectic A layer spacing

The smectic A layer spacing  $d$  has shown two kinds of behavior with *increasing pressure*:

(i) A *decrease* in layer spacing occurs when the smectic A phase is compressed toward the *stable solid transition* (e.g., Fig. 17). The change is small ( $\sim 1\%$ ). Table I shows  $\Delta d/d$  for two temperatures. The compressibility  $\beta$  has been measured for CBOOA by means of ultrasonic techniques.<sup>14</sup> Assuming it is independent of pressure, we can compute from it a relative volume change  $\Delta V/V$  and compare this to  $\Delta d/d$ . This we have also done in Table I in which we see that  $\Delta d/d \approx \Delta V/V$ , and not the one-third we would expect for an isotropic compressibility. This means that at these pressures the compressibility parallel to the layers is much smaller than that perpendicular to the layers when the smectic A phase is compressed toward a stable solid phase.

(ii) *No change* at all in the layer spacing when the smectic A phase is compressed toward the *reentrant phase* (e.g., Figs. 7–12). Even though there is no change in the layer spacing, the fact that the bulk compressibility is nonzero forces us to conclude that the lateral compressibility between molecules within the same layer is greater than the intralayer compressibility. Consequent-

TABLE I. Summary of the relative change in the smectic A layer spacing ( $\Delta d/d$ ) as a function of pressure from Fig. 17.  $\Delta V/V$ , the relative volume change, has been computed from the compressibility  $\beta$ , as measured by ultrasonic attenuation.<sup>14</sup>

$T$ (°C)	$\beta$ (kbar <sup>-1</sup> )	$\Delta V/V$ (%)	$\Delta d/d$ (%)
65.8	0.0495	0.61	0.87
69	0.0502	1.10	1.41

ly, the volume changes are such that the distance between nearest neighbors in the same plane decreases; this is in contrast to the behavior upon approach to the stable crystalline phase as cited above.

The molecules are packed in the layers in pairs which form antiparallel associations (see Fig. 2). With increasing pressure, we suppose that the number as well as the *lifetime* of each associated pair increases<sup>10</sup> just as it does with decreasing temperature. The antiparallel pairing neutralizes the long-range electrostatic forces envisaged as being responsible for binding the molecules into layers. When enough pairs have been created, the strength of the layers is weakened and they disintegrate into the reentrant nematic phase. Relaxing the constraint that the molecules lie in planes further allows for a denser packing of the molecules (see Fig. 2). In addition, as a function of time, the actual value of the layer spacing was observed to increase ( $\sim 3\%$ ), although the qualitative details of the relative change for any given run remained the same (Fig. 10) as a function of pressure. Assuming it is not an impurity effect (difficult to justify, but in any case impurities tend to decrease the reentrant pressure, not increase it as seen here) a tentative explanation is that it is due to the elongation of the aliphatic chain when pressure is applied *perpendicular* to the layers (see Fig. 5) for a long period of time. Perhaps pressure applied continuously in this direction "irons out" the tails. The enhanced length of CBOOA would stabilize the smectic A phase to higher pressure, as we observe here. By the same token, continuously applying pressure parallel to the layer normals may lead to a systematic decrease in the layer spacing with a concomitant reduction in the reentrant pressure.

##### B. Is the reentrant nematic phase identical to the classical nematic phase?

From the evidence presented in Figs. 6, 7, 11–13, 15, and 16, the answer is *yes*. These data demonstrate that approaching the smectic A phase from the reentrant nematic side by decreasing the pressure is qualitatively similar to approaching the smectic A phase from the classical nematic phase by decreasing the temperature. The interesting question as to how the smectic A fluctuations develop as a function of decreasing pressure will have to wait for a much more precise experimental setup.

##### C. Crystallization above the reentrant nematic phase

As a final point, we emphasize that under pressure, the reentrant nematic phase crystallizes

to a solid with lattice parameters of 20 and 19 Å. This is reminiscent of the 19-Å crystalline phase observed in mixtures at 1 atm.<sup>7</sup> Unlike the 19-Å solid in mixtures, releasing the pressure or cooling results in this solid phase (we call it crystal B) transforming to the stable crystalline phase (crystal A lattice parameters ~25 Å) which subsequently melts at some lower pressure (or higher temperature).

As was also proposed for the 19-Å solid phase in mixtures, it may be that the spacing of crystal B is related to the distance between two antiparallel pairs as proposed in Fig. 2.

#### V. CONCLUSIONS

We have presented evidence that microscopically, the high-pressure reentrant nematic phase is identical to the classical nematic phase. We have found that the smectic A phase at pressures below the reentrant nematic phase is virtually incompressible in the direction parallel to the layers

normal. We have also found that the characteristic spacing of the high-pressure solid phase is 19–20 Å. As a function of decreasing pressure or temperature, this solid transforms to the stable low-pressure one with characteristic spacing of 25 Å. Before refining our techniques for measuring the reentrant nematic smectic A transition, we would like to be able to chemically characterize our samples more precisely. An anomalous increase in layer spacing with time may be due to a gradual elongation of the "molten" chains with constant applied pressure perpendicular to the layer normals.

#### ACKNOWLEDGMENTS

We thank J. Stamatoff and T. Bilash for the use of their x-ray facilities. We also thank K. Miyano for stimulating discussions. W. B. Daniels acknowledges NSF grant (DMR 78-01-307) for partial support of this work.

---

\*Present address: Centre de Recherches sur les Macromolécules, Strasbourg, Fr.

<sup>1</sup>P. E. Cladis, *Phys. Rev. Lett.* **35**, 48 (1975).

<sup>2</sup>P. E. Cladis, R. K. Bogardus, W. B. Daniels, and G. N. Taylor, *Phys. Rev. Lett.* **39**, 720 (1977).

<sup>3</sup>N. Clark, *J. Phys. (Paris)* **40**, C3-345 (1979); D. D. Klug and E. Whalley, *J. Chem. Phys.* **71**, 74 (1979).

<sup>4</sup>P. S. Pershan and J. Prost, *J. Phys. (Paris)* **40**, L27 (1979).

<sup>5</sup>B. Deloche, B. Cabane, and D. Jerome, *Mol. Cryst. Liq. Cryst.* **15**, 197 (1971).

<sup>6</sup>P. H. Keyes, H. T. Weston, W. J. Lin, and W. B. Daniels, *J. Chem. Phys.* **63**, 5006 (1975).

<sup>7</sup>D. Guillon, P. E. Cladis, and J. Stamatoff, *Phys. Rev. Lett.* **41**, 1598 (1978).

<sup>8</sup>A. S. Roshamwala and R. Shashidhar, *J. Phys. E* **10**, 180 (1977).

<sup>9</sup>C. Druom and J. M. Wacrenier, *Ann. Phys. (Paris)* **3**, 199 (1978).

<sup>10</sup>P. E. Cladis, R. K. Bogardus, and D. Aadsen, *Phys. Rev. A* **18**, 2292 (1978).

<sup>11</sup>J. B. Stamatoff, T. Bilash, and Y. Ching (unpublished).

<sup>12</sup>F. Kahn, *Appl. Phys. Lett.* **22**, 386 (1973).

<sup>13</sup>W. L. McMillan, *Phys. Rev. A* **6**, 936 (1972).

<sup>14</sup>F. Kiry and P. Martinoty, *J. Phys. (Paris)* **39**, 1019 (1978).